Using biochar for environmental recovery and boosting the yield of valuable non-food crops: the case of hemp in a soil contaminated by potentially toxic elements (PTEs)

Heliyon 10 (2024) e28050

Contents lists available at ScienceDirect

Heliyon

journal homepage: www.cell.com/heliyon

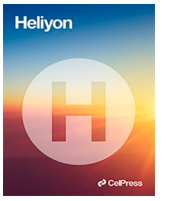

Research article

Using biochar for environmental recovery and boosting the yield of valuable non-food crops: The case of hemp in a soil contaminated by potentially toxic elements (PTEs)

Matteo Garau [a,1], Mauro Lo Cascio [a,b,1], Sotirios Vasileiadis [c], Tom Sizmur [d], Maria Nieddu [a], Maria Vittoria Pinna [a], Costantino Sirca [a,b], Donatella Spano [a,b], Pier Paolo Roggero [a,e], Giovanni Garau [a,*], Paola Castaldi [a,e]

[a] Dipartimento di Agraria, University of Sassari, Viale Italia 39, 07100, Sassari, Italy
[b] CMCC – Euro-Mediterranean Center on Climate Change Foundation, IAFES Division, Via de Nicola 9, 07100, Sassari, Italy
[c] Department of Biochemistry and Biotechnology, University of Thessaly, Greece
[d] Department of Geography and Environmental Science, University of Reading, Reading, RG6 6DW, UK
[e] Nucleo Ricerca Desertificazione, University of Sassari, Sassari, Italy

ARTICLE INFO

Keywords:
Antimony
Gentle remediation options
Microbial abundance
Microbial diversity
Cannabis sativa
PTEs-uptake

ABSTRACT

Hemp (*Cannabis sativa* L.) is known to tolerate high concentrations of soil contaminants which however can limit its biomass yield. On the other hand, organic-based amendments such as biochar can immobilize soil contaminants and assist hemp growth in soils contaminated by potentially toxic elements (PTEs), allowing for environmental recovery and income generation, e.g. due to green energy production from plant biomass. The aim of this study was therefore to evaluate the suitability of a softwood-derived biochar to enhance hemp growth and promote the assisted phytoremediation of a PTE-contaminated soil (i.e., Sb 2175 mg kg^{-1}; Zn 3149 mg kg^{-1}; Pb 403 mg kg^{-1}; and Cd 12 mg kg^{-1}). Adding 3% (w/w) biochar to soil favoured the reduction of soluble and exchangeable PTEs, decreased soil dehydrogenase activity (by ~2.08-fold), and increased alkaline phosphomonoesterase and urease activities, basal respiration and soil microbial carbon (by ~1.18-, 1.22-, 1.22-, and 1.66-fold, respectively). Biochar increased the abundance of selected soil culturable microorganisms, while amplicon sequencing analysis showed a positive biochar impact on α-diversity and the induction of structural changes on soil bacterial community structure. Biochar did not affect root growth of hemp but significantly increased its aboveground biomass by ~1.67-fold for shoots, and by ~2-fold for both seed number and weight. Biochar increased the PTEs phytostabilisation potential of hemp with respect to Cd, Pb and Zn, and also stimulated hemp phytoextracting capacity with respect to Sb. Overall, the results showed that biochar can boost hemp yield and its phytoremediation effectiveness in soils contaminated by PTEs providing valuable biomass that can generate profit in economic, environmental and sustainability terms.

* Corresponding author. Viale Italia 39, 07100, Sassari, Italy.
E-mail address: ggarau@uniss.it (G. Garau).
[1] These authors contributed equally to this work.

https://doi.org/10.1016/j.heliyon.2024.e28050
Received 13 December 2023; Received in revised form 11 March 2024; Accepted 11 March 2024
Available online 12 March 2024

1. Introduction

In the last decades, the exploitation of mineral and energy resources and the steady increase of non-renewable energy consumption substantially contributed to environmental pollution and climate change [1]. Renewable energy production, in particular bioenergy, can replace part of the energy produced by fossil fuels, e.g. through the production of plant biomass that can be burnt to generate heat and electricity or turned into biofuels. However, such use of land can divert productive soil from producing food or feed and negatively impact the food supply chain [1]. This is worrying, especially in light of recent global food demand estimates, which are expected to increase by 30 and 62% between 2010 and 2050 [2].

Soils contaminated by potentially toxic elements (PTEs such as Cd, Pb, Cu, Zn, As, and Sb), which cannot be used for cultivation of food or feed crops, and which require remediation, could be suitable for growing energy crops [3]. Mining activities represent one of the main sources of PTEs pollution of the environment, and PTEs released from abandoned mining sites are responsible for worsening soil physico-chemical properties, reducing microbial abundance, diversity and activity, as well as plant growth [4]. This is due to the high concentration of labile PTEs in soil (water soluble and easily exchangeable PTEs), which exerts a toxic action towards microbial communities and plants, and represents a severe risk for human health [4] (Enyigwe et al., 2022). Among the various PTEs, antimony (Sb) is a highly toxic emerging contaminant whose concentration in soil is continuously increasing [5] (Tang H et al., 2022). This element is readily absorbed by plants, causing a severe reduction in biomass production. Sb stress lowers chlorophyll synthesis, causes ROS production and MDA accumulation, harms chloroplast structure and leads to ultrastructural changes in plants [5]. Bioavailable Sb can also critically impair soil functionality by affecting the composition, size, and activity of resident microbial communities [6]. Reducing the concentration of labile PTEs and improving the physico-chemical and microbial characteristics of soil is therefore essential to mitigate ecotoxicological effects in such polluted areas and promote plant growth.

Assisted phytoremediation can be employed as an environmental and economic win-win strategy combining PTEs immobilization and the production of valuable non-food crops. Such green environmental technology combines the use of selected amendments and plant species for the immobilization of labile PTEs in rhizosphere or roots (phytostabilisation) or for their translocation into the aerial part (phytoextraction) (Lebrun et al., 2018). Biochar, the carbonaceous material rich in aromatic carbon produced by the pyrolysis biomass at high temperatures (i.e., 300–800 °C), is a promising amendment for assisted phytoremediation. Biochar is commonly characterised by alkaline pH, substantial amount of Fe (hydr)oxides, high specific surface area and by the presence of hydroxyl, ester, amino, carboxyl and carbonyl functional groups [7]. Due to these features, biochar can be effective in immobilizing different PTEs through precipitation reactions, complexation, and ion exchange processes [8] which reduce their bioavailability and the risk of PTEs spreading into the environment. However, biochar effectiveness can vary depending on the feedstock, the amount added, PTEs present in soil, and soil type. For instance, Zhu et al. [9] reported that biochar alleviated Sb stress on maize plants reducing its accumulation in shoot and root to shoot translocation. Jia et al. [10] and Wang et al. [11] reported that adding Fe- and Mn-modified biochar immobilized Sb in a contaminated soil and reduced its potential bioavailability to plants. On the contrary, further studies indicated that biochar addition increased the mobility and bioavailability of Sb [12], and El-Naggar [13] did not recommend biochar for the recovery of soils contaminated by multiple PTEs, e.g. As, Cd, Pb, and Zn. Moreover, Hussain et al. [14] recorded substantial Zn mobilization and uptake by mustard in polluted soils treated with different biochars, and Tsai et al. [15] also found significant mobilization of Cr, Cu, and Ni in a multi contaminated rural soil amended with poultry litter biochar. Taken together, these studies indicate that biochar impact on PTEs-contaminated soils can be variable, and a case-by-case assessment is needed before including this amendment in specific (phyto)remediation programs.

The plant species selected for phytoremediation should be robust and fast growing and should contribute to reducing labile PTEs in soil by means of their fixation in roots or aboveground biomass [6]. Identifying plant species that, in addition to these attributes, allow the production of valuable biomass suitable for green energy production and/or for different uses generating an income could make phytoremediation an effective environmental and economic intervention.

Hemp (*Cannabis sativa* L) is a particularly interesting option for phytoremediation because its biomass can be used for bioenergy production [3], wood fibre, pulp and fodder [16], and its seeds are also an excellent source of valuable oil [17,18]. Hemp has been used to clean up soils contaminated by pesticides, solvents, explosives, crude oil, polyaromatic hydrocarbons and toxins [16]. This Cannabaceae plant is fast growing, has wide and deep roots, can adapt to different soil conditions and grow in a variety of climates [16]. Citterio et al. [17] and Deng et al. [19] reported that hemp tolerates high concentrations of PTEs (i.e., Cd, Cr, Ni, and Pb), which are preferentially stored in roots and poorly translocated to the aboveground part. In contrast, Meers et al. [20] highlighted hemp as an ideal crop to remove PTEs from soil and translocate them into the shoots. Ćaćić et al. [21] tested different varieties of hemp grown in PTEs-contaminated soils, which behaved as hyperaccumulating (for Cd, Hg, Mo and Zn) or phytostabilising (for As, Co, Cr, Cu, Ni, and Pb) plants.

Overall, these studies highlight the general ability of hemp to grow in PTEs-contaminated soils even if its behaviour as phytostabiliser or phytoextracting species is rather unclear. Moreover, the growth response of hemp in PTEs-contaminated soils with high Sb concentrations typical of Sb mining sites is essentially unknown, and no studies have investigated so far the biochar - hemp interaction in such polluted soils.

This study aimed to evaluate the suitability of biochar and hemp in assisted phytoremediation programs for soils contaminated with Sb and other PTEs. More specifically, the following aspects were investigated in this study: i) the biochar influence on labile PTEs in an Sb-rich contaminated mining soil and its impact on several soil (bio)chemical and microbial endpoints (soil nutrient availability, basal respiration, dehydrogenase, urease and β-glucosidase activities, microbial counts, Biolog community level physiological profile, bacterial community diversity); ii) the biochar influence on hemp growth and yield in the same Sb-rich contaminated soil and on its phytoremediation potentials (i.e., PTEs uptake in shoots/seeds and roots and PTEs mineralomasses).

2. Materials and methods

2.1. Origin of contaminated soil, sampling and experimental set-up

Soil samples were collected in the proximity of the Su Suergiu ex-mining area (Cagliari) in Southeastern Sardinia (Italy), where stibnite (Sb_2S_3) was the main mineral extracted, with calcite ($CaCO_3$) and quartz (SiO_2) as impurities [22]. For many years it was the most important mine in Italy for the extraction of antimony. Mining residues (i.e., slag and tailings 87%, and waste rock 13%), containing substantial Sb concentrations and other PTEs as impurities, were accumulated and abandoned nearby the mining facility, spreading the pollutants in the surrounding soils and waters without effective interventions to mitigate their environmental impact [22]. For this reason, the soils sampled were expected to contain high Sb concentrations and other PTEs. As such, they are representative of many areas affected by Sb and PTEs pollution that can be found worldwide.

Soil samples (0–30 cm depth; n = 60, approx. 5 kg each) were randomly collected at February 2021, in proximity to the Sb smelting plant (39°29′N; 09°39′9E) in an area over approximately 1 ha. According to the World Reference Base for Soil Resources [23], the soil is classified as Lithic Leptosol (Arenic, Pyric, Technic, Toxic). Soil samples, bulked together, air-dried and sieved to <2 mm, were used to set up mesocosms. Particle size analysis identified the soil as sandy (USDA classification; i.e. 90.08% sand; 2.66% silt and 7.26% clay). The soil samples were divided into two subsamples, each of which was further divided into 3 mesocosms of approx. 50 kg each. Triplicate mesocosms were amended with 3% (w/w) biochar sieved to <2 mm (C + B treatment) or left unamended as control (C treatment). The biochar used as amendment was provided by Ronda SpA (Zanè, Italy) and derived from the pyrolysis of beech, poplar, and elder softwood at 700 °C. The biochar characteristics have been reported elsewhere [24] and are resumed in Table S1.

After biochar addition, treated and untreated soils were thoroughly mixed, soil water content (SWC) was maintained in the range of 20–25%, and soil temperature (Ts) between 25 and 35 °C. Mesocosms were incubated for 2 months at 20 °C, mixed once per week, and the SWC was maintained.

SWC in mesocosms was continuously monitored using moisture probes (ECH_2O, Decagon Devices Inc., Pullman, USA) connected to external data loggers (Em50 Data Logger, Decagon Devices Inc., Pullman, USA).

2.2. Physicochemical characteristics of soil

At the end of the incubation period, the main physicochemical characteristics of soil mesocosms were determined. Soil pH and electric conductivity (EC) were quantified on 1:2.5 (w/v) soil:water suspensions [25] (Table 1). Dissolved organic carbon (DOC) was determined following Manzano et al. [24], total organic C and N were quantified with a CHN analyzer (Leco CHN628) and Soil LCRM Leco part n° 502–697 as calibration sample. Extractable P was quantified with the Olsen method [25], while CEC and exchangeable bases (i.e., Na, Ca, K, Mg) were determined with the $BaCl_2$-triethanolamine method [25].

The pseudo-total concentration of PTEs (i.e., Cd, Cr, Cu, Ni, Pb, Sb, and Zn) was determined by an Inductively Coupled Plasma Optical Emission Spectrometer (PerkinElmer Optima 7300 DV ICP-OES) after microwave digestion (ultraWave Microwave Milestone) of soil samples (0.2 g) with 2 mL of suprapure H_2O_2, and 4 mL of a HNO_3 + HCl (3:1 v/v ratio) mixture. The NIST-SRM 2711 certified reference soil was included for quality assurance, with PTE recoveries between 8.5 and 10% of the certified values. The detection limits of the analyzed elements were between 2.63 μg L^{-1} (As) and 0.14 μg L^{-1} (Cd).

Table 1
Chemical properties of the untreated (C) and biochar-treated (C + B) contaminated soils (mean ± SE; n = 9).

	C	C + B
pH	7.31 ± 0.06[a]	7.90 ± 0.03[b]
EC (mS cm^{-1})	2.23 ± 0.06[a]	2.12 ± 0.08[a]
Organic matter (%)	6.31 ± 0.02[a]	9.85 ± 0.67[b]
Total organic C (%)	3.66 ± 0.01[a]	5.71 ± 0.39[b]
Total N (%)	0.29 ± 0.01[a]	0.30 ± 0.01[a]
DOC ($mg \cdot g^{-1}$)	3.49 ± 0.15[b]	1.58 ± 0.07[a]
P available ($mg \cdot kg^{-1}$)	7.23 ± 0.67[a]	17.41 ± 0.75[b]
Cation Exchange capacity (CEC, $cmol_{(+)} \cdot kg^{-1}$)	16.72 ± 0.02[a]	20.06 ± 0.70[b]
Exchangeable Na ($cmol_{(+)} \cdot kg^{-1}$)	0.97 ± 0.22[a]	1.05 ± 0.03[a]
Exchangeable K ($cmol_{(+)} \cdot kg^{-1}$)	1.72 ± 0.02[a]	1.62 ± 0.09[a]
Exchangeable Ca ($cmol_{(+)} \cdot kg^{-1}$)	14.53 ± 0.95[a]	16.44 ± 0.98[a]
Exchangeable Mg ($cmol_{(+)} \cdot kg^{-1}$)	2.25 ± 0.18[a]	2.65 ± 0.22[a]
Pseudo-total PTEs ($mg \cdot kg^{-1}$)		
Cd	11.91 ± 1.33[a]	12.52 ± 3.05[a]
Cr	47.12 ± 1.99[a]	85.29 ± 22.32[b]
Cu	136.18 ± 4.74[a]	135.93 ± 3.37[a]
Ni	122.02 ± 9.56[a]	131.46 ± 11.60[a]
Pb	402.96 ± 6.34[a]	391.98 ± 5.53[a]
Sb	2174.95 ± 122.48[a]	2128.03 ± 119.20[a]
Zn	3148.92 ± 177.66[a]	2918.19 ± 71.46[a]

Mean values followed by different letters denote statistically significant differences according to the Fisher's LSD test ($P < 0.05$).

2.3. PTEs mobility in soil mesocosms

Only the mobility of those PTEs whose concentration exceeded the contamination thresholds established by the Italian regulations [26], i.e., Sb, Cd, Pb, and Zn (Table 1), was assessed.

To quantify the Sb mobility in soil mesocosms (after the incubation period), the sequential extraction of Wenzel et al. [27] was used. In brief, the following Sb fractions were quantified: the water-soluble and non-specifically sorbed Sb (Fraction 1; extracted with a 0.05 M $(NH_4)_2SO_4$ solution); the specifically sorbed Sb (Fraction 2; extracted with a 0.05 M $NH_4H_2PO_4$ solution); the Sb bound to amorphous and poorly crystalline Fe and Al hydroxides (Fraction 3; extracted with a 0.2 M NH_4^+-oxalate buffer solution); the Sb bound to well-crystallized Fe and Al hydroxides (Fraction 4; extracted with a 0.2 M NH_4^+-oxalate buffer+ 0.1 M ascorbic acid solution). Additional methodological details can be found elsewhere [28].

The sequential extraction of cationic PTEs was carried out following the protocol described by Basta and Gradwohl [29]. In brief, the following PTEs fractions were quantified: the water-soluble and readily exchangeable PTEs (Fraction 1; extracted with a 0.5 M Ca $(NO_3)_2$ solution); PTEs forming weak surface complexes (Fraction 2; extracted with a 1 M NaOAc solution at pH 5.0); surface complexed and precipitated PTEs (Fraction 3; extracted with a 0.1 M Na_2EDTA solution). Additional methodological details can be found elsewhere [30].

The residual PTEs fractions were determined, for both the sequential extraction procedures, after the mineralization of the soil samples resulting from the different extraction with 2 mL of suprapure H_2O_2 and 4 mL of a mixture of HNO_3 + HCl (3:1 v/v ratio), and microwave digestion (ultraWave Microwave Milestone). The PTEs present in each liquid fraction were quantified by ICP-OES (PerkinElmer Optima 7300 DV ICP-OES). The NIST-SRM 2711 certified reference soil was included for quality assurance, with PTE recoveries between 8.5 and 10% of the certified values. The detection limits of the analyzed elements were between 2.63 μg L^{-1} (As) and 0.14 μg L^{-1} (Cd).

2.4. Enzyme activities, soil basal respiration and microbial carbon

After incubation, selected biochemical and microbiological characteristics were determined in soil mesocosms. In particular, the dehydrogenase (DHG), urease (URE), β-glucosidase (GLU), and acid and alkaline phosphomonoesterase (PHA and PHB) activities were quantified colorimetrically following the procedures described by Alef and Nannipieri [31].

To monitor soil basal respiration (CO_2 efflux), two polyvinyl chloride (PVC) collars (20 cm inner diameter) were placed in each mesocosm (n = 12 total PVC collars), and CO_2 efflux was quantified for each collar with a portable Li-8100 (LI-COR Inc., Lincoln, NE, USA). Measurements took 105 s per collar and were taken weekly throughout the incubation time between 5:00 and 7:00 p.m. (local time, GMT + 1) to avoid direct radiation from reaching the collars and to minimize soil temperature variability during sampling. The temperature at a 5 cm depth adjacent to the collars was recorded simultaneously with CO_2 efflux measurements using a probe connected to the LI-COR 8100. Each collar's headspace was measured and considered to quantify CO_2 efflux rates as μmol CO_2 m^{-2} s^{-1}.

After soil incubation with biochar, soil microbial biomass C (SMB-C) was quantified in triplicate soil aliquots (40 g) from each mesocosm using the chloroform fumigation extraction method as previously reported [32]. Briefly, 20 g of each soil sample were fumigated in the dark at 25 °C with ethanol-free chloroform for 24 h, while the remaining 20 g were directly extracted with 80 mL of 0.5 M K_2SO_4 for 1 h (orbital shaker, 40 rpm). The same extraction procedure was applied to chloroform-fumigated samples after chloroform evaporation in a fume hood. All soil extracts were centrifuged and UV absorbance at 280 nm (A_{280}) measured.

2.5. Community-level physiological profile, culturable microorganisms, and molecular analysis of soil bacterial community

After the incubation time, the community-level physiological profile (CLPP) of soil microbial communities was obtained for each mesocosm by means of Biolog EcoPlates (Biolog Inc., Hayward, CA). The protocol described by Garau et al. [6] was followed to extract microbial communities from the different soil sample and subsequent inoculation into the Biolog EcoPlate wells (i.e., a 96-wells microtiter plate containing a sole C source in each well, and a control well with no C, and three replicated wells per C source). The tetrazolium violet present in each well allows the monitoring C source consumption which was recorded every 24 h by measuring the optical density of each well at 590 nm (OD_{590}). Principal component analysis (PCA) was carried out (using the correlation matrix) on the normalized OD_{590} values [6] to reduce multidimensional data and allow for easier interpretation of C source consumption data. Percent utilization of the different C source guilds within each Biolog EcoPlate (sugar and sugar derivates, sugar phosphates, carboxylic acids, amino acids, polymers) was also determined. Data related to C source consumption and PCA analysis refer to the 96-h time, since this time point allowed for the best treatment's distinction.

After the incubation period, total culturable heterotrophic bacteria, actinomycetes, fungi, and heat-resistant bacterial spores (e.g., *Bacillus* spp.) were quantified in soil mesocosms using the ten-fold serial dilution and spread plate method previously described [33]. To quantify the different microbial populations the following growth media were used: AIA (Actinomycete Isolation Agar, Difco, Milan, Italy) for actinomycetes; 1:10 TSB (Tryptic Soy Broth, Microbiol, Cagliari, Italy) + agar (1.5%) for soil heterotrophic bacteria and aerobic bacterial spores; GYEP pH 4.7 (Glucose Yeast Extract Peptone medium) for soil fungi. Microbial counts were conducted after incubation of the plates at 25 °C for 72 h and reported as Log_{10} CFU (Colony Forming Unit) g^{-1} soil (dry matter basis).

DNA was extracted from each soil sample (~500 mg) with the PowerSoil DNA isolation kit (Mo Bio laboratories, Carlsbad, CA). DNA extracts were used as templates for PCR amplification of the V4–V5 (primer-set: 515f 5′-GTGYCAGCMGCCGCGGTAA-3′, 926r 5′-CCGYCAATTYMTTTRAGTTT-3′) regions of the 16S rRNA gene [34,35], and 300bp paired-end sequencing was carried out at the Integrated Microbiome Resource (IMR, Halifax, NS, Canada) facilities according to their in-house protocol [36].

The sequencing data can be accessed with the Bioproject number PRJNA930723 at the Sequence Read Archive of the National Center for Biotechnology Information (https://www.ncbi.nlm.nih.gov/bioproject/).

2.6. Bioinformatics data analysis

Sequencing data were quality assessed and controlled, and microbial sample to amplicon sequence variant (ASV) matrices were generated with the dada2 v1.22.0 package [37] of the R v4.1.3 software, based on previously published protocols [38] as follows. Data were quality assessed and sequences with unknown nucleic acid bases were removed. Sequencing error rates were estimated and read-pairs were assembled to their amplicons of origin. Read-pairs with mismatches at the '3-end (error prone) read areas, preventing the reconstruction of the original sequences, were removed from downstream analysis. Chimeric amplicons (according to de novo chimera search) and off-target sequences (based on taxonomic annotation with the Silva v138 16S rRNA gene database; [39]) were also removed.

2.7. Pot experiment and plant analysis

At the end of soil-biochar incubation, six pots (40 cm diameter, 30 cm height), each containing about 25 kg of soil, were set up for each treatment (two for each mesocosm); 12 pots in total were therefore arranged. Twenty hemp plantlets (*C. sativa* L.) cv. Tiborszallasi were initially planted in each pot and thinned to 6 after 2 weeks. Plants were cultivated for 5 months (from April to September 2022) in a greenhouse under controlled conditions (25–35 °C air temperature and 60–70% relative humidity). The experiment was stopped when plant seeds were fully mature. At harvest, seeds, shoots and roots were separated, carefully and vigorously washed with deionized water, to effectively remove adhering soil particles from the roots, and dried at 55 °C for 72 h; then plant tissues were mineralized by microwave digestion (ultraWave Microwave Milestone) with a solution containing 2 mL of suprapure H_2O_2 and 4 mL of a mixture of HNO_3 and ultrapure H_2O (ratio 1:1). Afterwards, total PTEs concentration (i.e., Sb, Cd, Pb and Zn) in mineralized roots, shoots and seeds samples was determined by ICP-OES (PerkinElmer Optima 7300 DV). Peach leaves (NIST-SRM 1547) were used as standard reference material for quality assurance, with PTE recoveries between 8.5 and 10% of the certified values. The detection limits of the analyzed elements were between 2.63 μg L^{-1} (As) and 0.14 μg L^{-1} (Cd).

The root (MM_R), shoot (MM_A), and seed (MM_S) PTE mineralomasses were calculated as roots, shoots, or seeds biomass x PTE concentration in roots, shoots, or seeds [40].

2.8. Data analysis

All the chemical, biochemical and microbial analyses were carried out on triplicate (independent) soil samples collected from each mesocosm, while plant analyses were conducted on triplicate plant samples for each pot. All the data used to generate Figures and Tables have been included as supplementary material (Suppl. Data). Tables and figures report mean values ± standard errors (SE). Mean values from the different treatments were compared by One-way Analysis of Variance (ANOVA) followed, when significant *P*-values ($P < 0.05$) were obtained, by the post-hoc Fisher's least significant difference test (LSD, $P < 0.05$). Statistical analyses were carried out using the NCSS 2007 Data Analysis software (v. 07.1.21; Kaysville, Utah). Considering that soil basal respiration measurements were repeated over the incubation time, a general linear mixed model (GLMM) was used to compare the treatments. GLMM was performed in R using the "lme4" package. Time measurement and the experimental design were included in the model as random factors (Table S2).

Regarding the bioinformatic data, the generated ASV matrices were used for α/β-diversity analysis. The vegan v2.6-2 [41] (Oksanen et al., 2020) R package was used for calculating the richness (S) and the ACE [42] richness estimator (representative of identified/estimated number of ASVs, or, zero order diversity), the Shannon index (representative of less dominant ASVs or 1st order diversity), the reciprocal Simpson index (indicative of more dominant ASVs or 2nd order diversity) [43], and Fisher's α [44] (indicative of the highly dominant ASV diversity). These α-diversity indices were subjected to Student's t-tests or the non-parametric equivalent of the Wilcoxon rank sum test (in cases where *t*-test conditions were not met). The ASV matrices were agglomerated into genus level, and genera identified in all three treatment replicates were retained for the β-diversity analysis. Permutational multivariate analysis of variance (PERMANOVA) and non-metric multidimensional scaling (NMDS) were performed with the vegan package to assess possible biochar effect on soil microbial communities. Differential abundance of genera between the two treatment levels was assessed with the Fischer's exact test after *P*-value adjustment with the Benjamini-Hochberg method using the edgeR v3.36.0 R package. Taxa with significantly different counts are presented as a heatmap with hierarchical clustering using the complete linkage algorithm.

3. Results and discussion

3.1. Influence of biochar on the chemical properties of the contaminated soil

The main chemical characteristics of the untreated and biochar-treated soils are reported in Table 1. Due to biochar alkalinity (Table S1), its addition led to a pH increase of approx. 0.6 units compared to control soil, while EC, total N, and exchangeable bases were not affected (Table 1). Differently, CEC increased by 1.20-fold in biochar-treated soil *vs* control. Despite a ~1.56-fold increase of total organic C in biochar-treated soil, the DOC content decreased by 2.21-fold in this latter soil compared to control, confirming that

biochar C was mostly recalcitrant and insoluble as previously reported [24]. The DOC decrease in the amended soil could have been due to: i) H-bonding between biochar functional groups (-OH and –COOH) and DOC molecules, and π–π interactions; ii) pore-filling mechanism and hydrophobic interactions [24]. The high content of available P in biochar (Table S1) can partly explain its significant increase in the amended soil (+2.41-fold) compared to the control (Table 1). The pseudo-total concentration of Sb, Pb, Zn and Cd in the untreated soil was higher than threshold values established by the Italian legislation for agricultural soils, i.e. 10, 100, 300 and 5 mg kg^{-1} respectively [26]. Biochar addition did not change the concentration of pseudo-total PTEs in soil.

Overall, biochar addition improved soil chemical characteristics (P availability and CEC in particular), confirming its potential for the revegetation of PTEs-contaminated soils. However, such potential should be proven experimentally in specific plant growth experiments.

3.2. *Influence of biochar on Sb mobility*

The results of the sequential extractions showed that in the untreated soil, the percentage of water-soluble and exchangeable Sb (i.e., the labile Sb fraction, Fraction 1), although low compared to the pseudo-total Sb concentration in soil (i.e., 0.65%, Fig. 1A), was very high in absolute terms (>10 mg kg^{-1}). Labile Sb decreased by 1.14-fold after biochar addition (Fig. 1A). This is relevant from an environmental viewpoint since this fraction is recognized to greatly impact soil functionality [27,30]. Moreover, from a remediation viewpoint, the 3% biochar addition led to a reduction of approx. 6 kg of labile Sb per ha (assuming 0.3 m depth; 1300 kg m^3 soil density) which is remarkable. This reduction can be attributed to the formation of more stable interactions between the $Sb(OH)_6^-$ oxyanion (the dominant Sb species in aerobic soils; [28]) with different functional groups of biochar such as hydroxyl groups [8], its occlusion within biochar pores, and/or its precipitation as insoluble compound [45]. The content of Sb chemically bound to biochar surfaces through inner-sphere complexes (Fraction 2, Fig. 1A) was 2.48% and 2.22% of the pseudo-total Sb in C and C + B soil respectively, with a 1.1-fold reduction in the amended soil. A similar trend was observed for the Sb associated to poorly crystalline and amorphous Fe and Al (hydr)oxides (Fraction 3, Fig. 1A). In particular, biochar addition decreased by 1.1 times the Sb extracted in Fraction 3. The Sb associated to well-crystallized Fe and Al oxides (Fraction 4, Fig. 1A) was not affected by biochar addition while the residual Sb (i.e. that strongly retained by soil colloids and/or precipitated) significantly increased in amended soil (Fig. 1A). This fraction was the most relevant in both soils, with ~47 and 49% of the pseudo-total Sb in C and C + B respectively (Fig. 1A). These results agree with Hua et al. [46], who reported a reduction of Sb labile pools and an increase of residual Sb in a contaminated soil treated with straw and apple tree-derived biochar. Wang et al. [11] also reported a reduction of Sb mobility in a contaminated soil treated with low rates (i.e. between 0.5 and 2%) of tea branches-derived biochar and Fe–Mn-modified biochar. On the whole, adding biochar favoured a redistribution of soil Sb, i.e. a reduction of soluble, exchangeable and chemically bound species and a parallel increase of more stable (and hardly bioavailable) ones. Such Sb immobilizing effect was attributable to the high concentration of metal cations in biochar (e.g. exchangeable Ca; Table S1), which could have favoured the formation of insoluble Ca–Sb precipitates, as well as to the presence of Fe and Mn oxides that can fix this PTE increasing its residual fraction [8,46,47].

Although the influence of biochar in reducing labile antimony was significant, substantial amounts of potentially bioavailable Sb

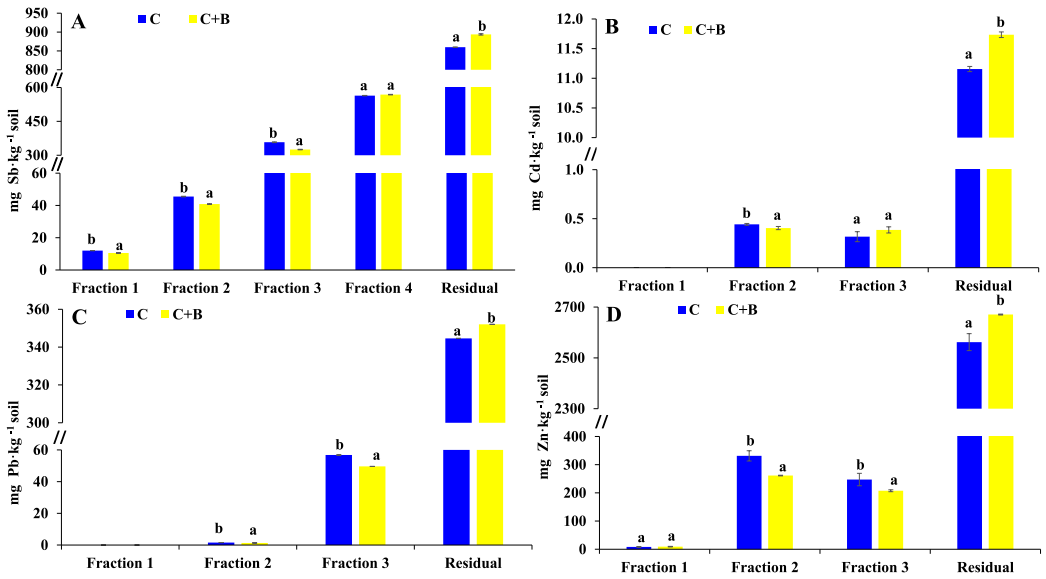

Fig. 1. Sb (A), Cd (B), Pb (C) and Zn (D) released after sequential extraction in biochar treated (C + B) and untreated (C) soils (mean ± SE; n = 9). For each PTE and within each fraction, different letters denote statistically significant differences between C and C + B according to the Fisher's LSD test ($P < 0.05$).

were still present in C + B treatment. The high mobility of the $Sb(OH)_6^-$ anion may still cause a serious threat to the abundance, diversity, and functionality of the soil microbial community as well as to the soil's fertility. These aspects should be carefully investigated in order to fully understand the biochar potentials to recover Sb-contaminated soils.

3.3. Influence of biochar on the mobility of cationic PTEs

The water-soluble and readily exchangeable Cd and Pb were under the detection limit (<0.2 μg kg^{-1}; Fraction 1, Fig. 1B and C), while labile Zn (Fraction 1, Fig. 1D) did not change after biochar addition. The concentration of Zn in Fraction 1 of treated and untreated soils was small compared to its pseudo-total concentration (0.26% and 0.29% in C and C + B soils, respectively; Fig. 1D). Probably, the neutral soil pH, and the use of charcoal during the smelting process [22] promoted the retention of soluble PTEs by the carbonaceous material through surface adsorption and internal diffusion processes. It is noteworthy to highlight that the low or no content of Cd, Pb and Zn in Fraction 1 implies a low environmental risk due to the high mobility and potential bioavailability (for plants and microorganisms) of this fraction [6,30].

The fractions of PTEs extracted with NaOAc (Fraction 2) were 3.71%, 0.38%, and 10.52% of the pseudo-total Cd, Pb, and Zn respectively. These fractions decreased by 1.09-, 1.18- and 1.27-fold for Cd, Pb and Zn respectively in the biochar-amended soil (Fig. 1B, C and D). The PTEs extracted in Fraction 3 (i.e., those poorly mobile and bioavailable) were 2.66, 14.10 and 7.85% of the pseudo-total Cd, Pb and Zn respectively (Fig. 1B, C and D). The EDTA-extractable (i.e., Fraction 3) Pb and Zn decreased by 1.15- and 1.19-fold in biochar-amended soil respectively compared to the control, while it remained unchanged for Cd. A significant increase of the residual Cd, Pb and Zn pool (+1.05-, +1.02- and +1.04-fold compared to C, respectively), which accounted for more than 80% of the pseudo-total PTEs concentration was recorded in biochar treated soil (Fig. 1B, C and D). The pH increase in the C + B soil, the high content of available P in biochar (which can favour the formation of stable PTEs precipitates, e.g. PTEs-phosphates), as well as the presence of amorphous Fe and Mn oxides and organic functional groups in biochar (e.g. carboxylic and phenolic) contributed to reduce the mobility of PTEs in the amended soil and to increase their residual fraction, in agreement with previous studies [24].

3.4. Influence of biochar on soil enzyme activities, microbial carbon and soil basal respiration

Soil enzyme activities (i.e., DHG, URE, GLU, PHA and PHB) are sensitive to environmental changes, such as pH variation or nutrient availability in soil [48]. However, they are also sensitive to PTEs, which could influence their activity (e.g., by denaturation or inactivation) and/or their abundance in soil (e.g., by exerting a toxic effect on soil microbial populations; [30,47]).

The DHG activity, due to intracellular enzymes whose activity is used to estimate the oxidative capability of soil microbial

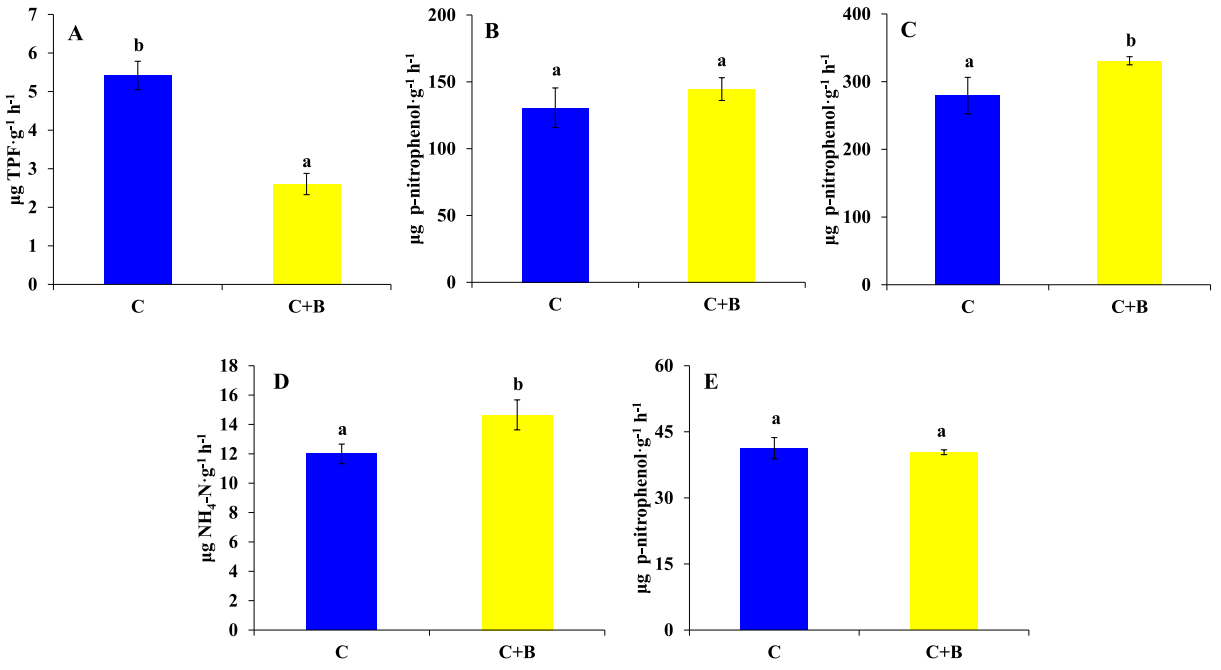

Fig. 2. Dehydrogenase (A), acid phosphomonoesterase (B), alkaline phosphomonoesterase (C), urease (D), and β-glucosidase (E) activity in biochar treated (C + B) and untreated (C) soils (mean ± SE; n = 9). For each enzyme activity, different letters indicate significant differences between C and C + B according to the Fisher's LSD test ($P < 0.05$).

communities [49], decreased by 2.1-fold in C + B soil compared to C (Fig. 2). This is in line with Demisie et al. [50] and Khan et al. [51], who observed a reduction of DHG activity in a soil treated with low rates (between 1 and 2.5%) of bamboo- and wheat straw-derived biochar. Likewise, Ali et al. [52] reported a reduction of DHG activity in a Zn and Cd polluted soil treated with 5 and 10% of apricot shell- and apple tree-derived biochar. Also, Kaurin et al. [53] observed reduced DHG activity in a Cd, Pb and Zn polluted soil treated with microbially enriched biochar. It is possible that the biochar used in this study, characterised by a high specific surface and adsorbing capacity [8,24], retained part of the triphenyl-tetrazolium chloride (TTC) or triphenylformazan (TPF) used to quantify DHG, leading to an underestimation of the enzyme activity in biochar-treated soil [54]. Alternatively, the reduced DHG activity could be due to a reduction of the microbial abundance in the amended soil which led to reduced DHG activity.

PHA and PHB activities in soil are due to extracellular enzymes released by soil microorganisms (and particularly sensitive to soil pH) that catalyse the hydrolysis of phosphate anhydrides and esters [31]. Biochar addition did not affect PHA, while PHB increased by

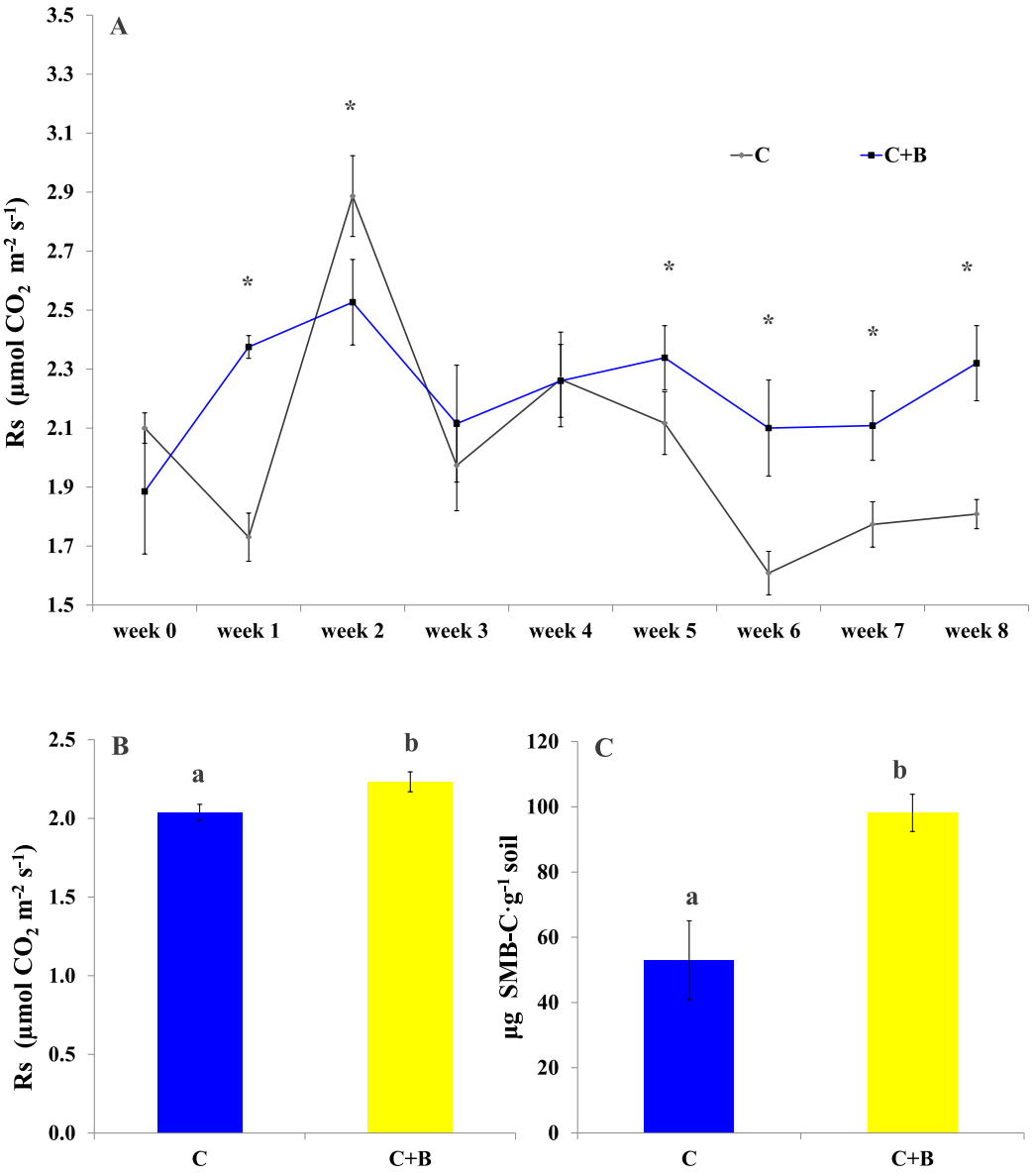

Fig. 3. Soil basal respiration (Rs; A), grand mean soil respiration (Rs; B), and soil microbial biomass carbon (SMB-C; C) in biochar treated (C + B) and untreated (C) soils (mean ± SE; n = 9). For soil basal respiration (A), asterisks (*) denote significant differences (for the same timepoint) between C and C + B according to the Fisher's LSD test ($P < 0.05$). For grand mean soil respiration (B) and soil microbial carbon (C), different letters denote statistically significant differences between C and C + B according to the Fisher's LSD test ($P < 0.05$).

1.18-fold in C + B soil compared to the control (Fig. 2). This could be explained by the different activity of PHA and PHB at different pH values, being the former more active at acid and sub-acid pH, and the latter at alkaline ones, like those recorded in C + B soil (Table 1; [55]).

URE activity, due to extracellular enzymes capable of catalysing the hydrolysis of urea to CO_2 and NH_4^+, increased by 1.22-fold in C + B compared to C (Fig. 2), in line with previous findings [52,55]. These authors reported an increase of URE activity in PTEs-contaminated soils treated with biochar from different sources (apricot shell, apple tree and corn stalk). In our case, this could be due to an increased microbial activity in the amended soil, resulting in increased synthesis of URE to meet the available nitrogen demand of the microbial community [55]. If it was the case, the reduced DHG activity recorded in C + B was therefore attributable to biochar adsorption of TTC and/or TPF.

GLU activity, which catalyses the hydrolysis of non-reducing terminal glucosyl residues from polysaccharides, was not affected by biochar addition (Fig. 2). This agrees with Ali et al. [52] who observed that biochar derived from apricots and apple trees, when applied at low doses (i.e., 1% or 2.5%), did not affect or slightly reduced GLU activity in Cd- and Zn-contaminated soils.

During the first 2 weeks of incubation soil basal respiration increased in both treatments (C and C + B) then steadily decreased (Fig. 3A). However, between week 5 and 8 respiration of C + B was always higher (approx. 1.22-fold) compared to C (Fig. 3A). Similar results were reported in a meta-analysis of 18 studies considering several types of biochar and soils, and were explained as a short-term "priming effect" of biochar [56]. The new source of C brought by the biochar addition may have increased CO_2 emissions in the amended soil, as evidenced by the grand mean of soil respiration (Fig. 3B). At the end of the incubation period, the SMB-C reflected a similar trend, i.e. it was 1.85-fold higher in C + B compared to C (Fig. 3C). It is likely that the reduction of labile PTEs (and consequent reduced bioavailability) resulted in a beneficial effect on the soil microbial community whose size and activity increased as evidenced by the SMB-C content and CO_2 emission data. This contrasts with the reduced DHG recorded in C + B soil, which, in light of these findings, can be explained by the TTC and/or TPF adsorption by the biochar rather than a reduced microbial content in the amended soil. These results showed that the studied biochar can increase soil microbial abundance and general activity while stimulating selected soil enzyme activities. It remained to clarify if this was also accompanied by a change of the soil microbial community structure.

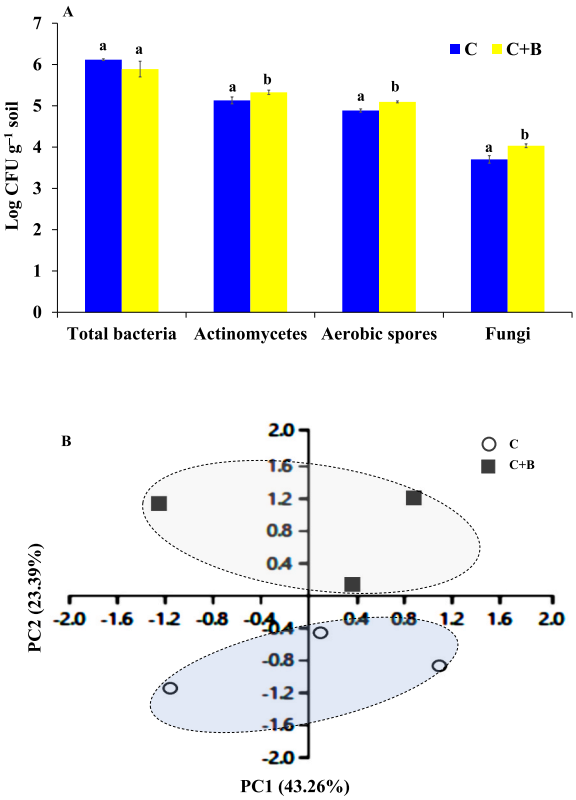

Fig. 4. Microbial counts (A) and biplot of the PCA scores (B) of biochar treated (C + B) and untreated (C) soils (mean ± SE; n = 9). For microbial counts (A), and within each microbial group, different letters denote statistically significant differences between C and C + B according to the Fisher's LSD test ($P < 0.05$).

3.5. Influence of biochar on culturable soil microbial communities and bacterial diversity

Apart for total culturable bacteria, whose decrease in C + B was not statistically significant, the size of the other targeted culturable microbial populations significantly increased (i.e., between 1.57- a 1.98-fold) in biochar amended soil (Fig. 4A). The reduced PTEs mobility (Sb especially) and the higher P availability recorded in the amended soil favoured the growth of culturable actinomycetes, fungi and spore-forming bacteria.

The Biolog CLPP highlighted a different use of C sources by the microbial communities of different soils. This was shown by the PCA analysis of carbon source utilization data (Fig. 4B) which accounted approx. for 67% of total variance and separated well C and C + B microbial communities. Tween 80 (r = 0.85), D-cellobiose (=0.86), D-glucosaminic acid (r = 0.98), D-malic acid (r = 0.83), L-phenylalanine (r = −0.82) and L-threonine (r = 0.86) were identified as the C sources highly correlated with PC1, while β-methyl-D-glucoside (r = 0.65), D,L-α-glycerol phosphate (r = 0.62), γ-hydroxybutyric acid (r = 0.66), itaconic acid (r = 0.88) and L-arginine (r = 0.81) were highly correlated with PC2. Overall, C + B microbial communities showed a higher utilization of carboxylic acids (i.e., +4%) and a reduced consumption of sugar and sugar derivates (i.e., −5%) compared to those of the unamended C soil (Table S3). These results pointed out that biochar not only led to an increase in size of the microbial community but also influenced its diversity.

The influence of the biochar on microbial diversity was investigated by the molecular DNA analysis of soil bacterial population. Quality assessment and quality control results are presented in Table S4. The analysis of α-diversity indices showed statistically significant differences between the two treatments in all dominance levels and corresponding indices, and indicated a clear role of biochar in the promotion of soil bacterial diversity (Fig. 5A).

NMDS results also showed a clear sample grouping according to the treatment, with the PERMANOVA results showing that 61.14%

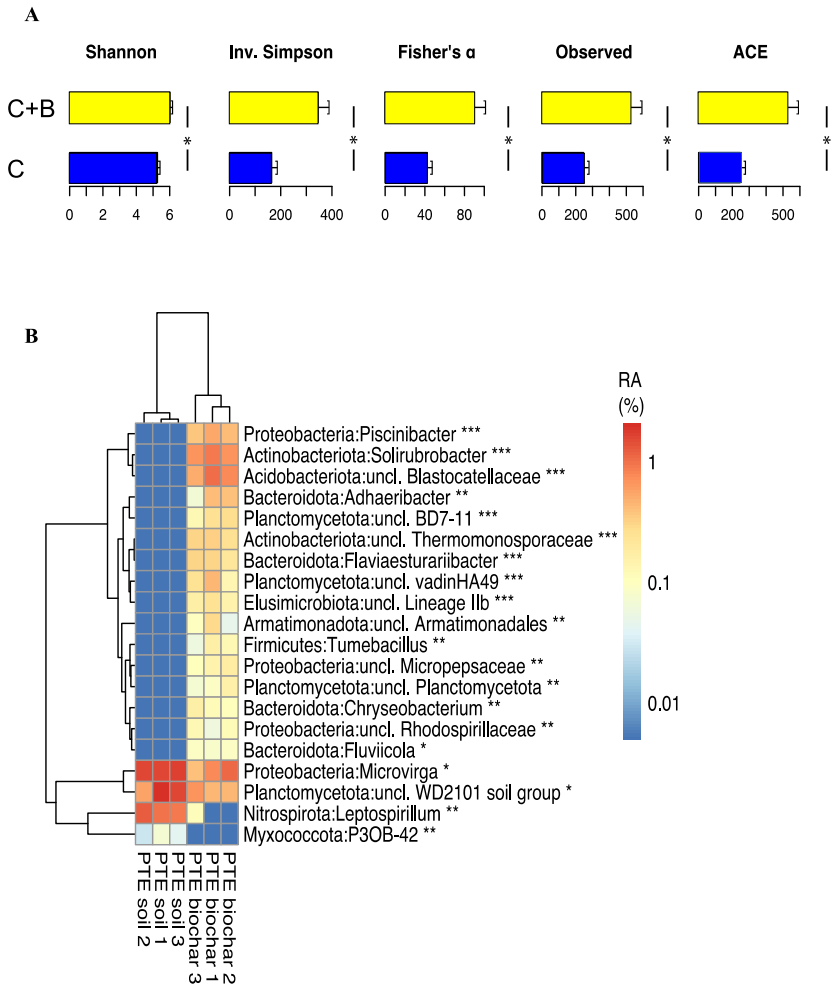

Fig. 5. Barplots (mean values ± SD) of the measured α-diversity indices (A) and heatmap with average linkage hierarchical clustering orders of identified differentially abundant taxa (B) in biochar treated (C + B) and untreated (C) soils. For each α-diversity index (A), asterisks denote statistically significant differences ($P < 0.05$) between C and C + B according to the Student's t-test or the non-parametric equivalent Wilcoxon rank-sum test. For the heatmap, phylum level taxonomy information is also provided for each taxon and asterisks indicate significant differences between C and C + B after *P-value* correction according to the Benjamini-Hochberg algorithm (*$P < 0.05$; **$P < 0.01$; ***$P < 0.001$).

of the observed variance coincided with the treatment groupings (Fig. S1). In the PERMANOVA model, although the R^2 was rather high (showing a strong effect along the treatment gradient), the model *P*-value was not significant ($P = 0.1$). However, it should be noted that the reason for this is purely technical since PERMANOVA requires at least 4 replicates for 2 treatment levels to enable *P*-values smaller than 0.05 [57].

Moreover, differential abundance analysis aiming to identify prevalent genera across treatments (present in all replicates of at least one treatment group), showed 20 genera being differentially abundant among treatments (Fig. 5B). Such analysis, as also suggested by NMDS, indicated a significant impact of biochar on the bacterial community composition. In particular, the abundance of selected *Proteobacteria*, *Actinobacteriota* and *Acidobacteriota* was stimulated by biochar while *Nitrospirota* and *Myxococcota* were significantly reduced (Fig. 5B). Overall, these results (Fig. 5) show that biochar derived from softwood was able to increase soil bacterial diversity and to significantly change the structure of the bacterial community inhabiting the PTEs-contaminated soil. This could be relevant in terms of plant growth as different authors highlighted a positive relationship between soil fertility and microbial diversity [58], while the influence of soil microbial community on plant growth is widely recognized [59]. However, these aspects need further evaluation and experimental evidence from specific plant growth experiments.

3.6. *Influence of biochar on hemp growth*

Hemp successfully grew in the PTEs-contaminated soil and no apparent phytotoxicity symptoms were detected. Biomass production of hemp grown in the polluted soil (Fig. S2) was similar to that observed by Cosentino et al. [60] and Flajšman and Kocjan Ačko [61], who cultivated the cv Tiborszallasi (the same used in our study) in uncontaminated agricultural soils. On the other hand, comparable shoot and seed biomass was also observed by Ref. [18] when cannabis (cv. USO 31) was grown in a Cd-, Ni- and Pb-contaminated soil; while higher biomass yields were reported by Meers et al. [20] for hemp (cv. Fibranova, Chameleon and Codimono respectively) grown in a multi-PTEs-contaminated soil where, however, Sb was not present. These results suggest that hemp variety can be relevant to optimize biomass production in PTEs-contaminated soils.

Biochar did not significantly affect root growth but did significantly increase cannabis aboveground biomass. Shoot biomass in C + B increased by 1.67-fold, and seed number and weight increased by ~2-fold compared to C (Fig. S2). The enhanced soil fertility (particularly due to the increase of the available P and CEC; Table 1), the reduced content of labile Sb and other PTEs, the higher soil microbial content (i.e., SMB-C) as well as the community structure and activity within biochar amended soil, were likely responsible for the higher yield of hemp in the amended soil. A positive impact of biochar on hemp biomass was previously observed by Loffredo et al. [62] for the cv. Kompolti (i.e., 78 and 59% for roots and shoots respectively) grown in a soil contaminated by organic pollutants. Apart from that, we are not aware of other studies addressing biochar impact on hemp growth in polluted soils. Overall, these results highlight that hemp can be successfully grown in soils heavily contaminated by Sb and other co-occurring PTEs and that biochar enhanced plant biomass in such harsh environments. This latter biomass could be used for bioenergy production and/or bio-based products (biofuels, bioplastics and fibres), thus opening the possibility of converting unproductive contaminated soils into exploitable and productive ones (e.g., Ref. [3]). However, the role of hemp as PTEs phytostabilizer or phytoextractant in such soils remains to

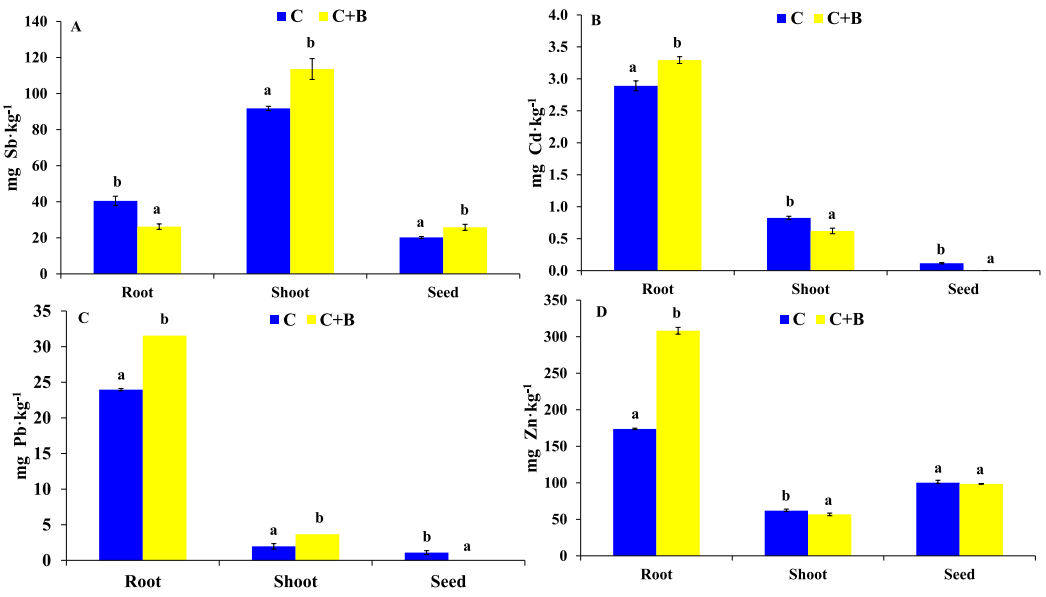

Fig. 6. Concentrations of Sb (A), Cd (B), Pb (C) and Zn (D) in roots, shoots and seeds of hemp grown on biochar treated (C + B) and untreated (C) soils (mean ± SE; n = 18). For each plant part, different letters denote significant differences between C and C + B according to Fisher's LSD test ($P < 0.05$).

be ascertained.

3.7. Influence of biochar on PTEs uptake by hemp

Apart from Sb, the other PTEs (i.e. Cd, Pb and Zn) were mainly concentrated in root tissues, regardless of the treatment applied (Fig. 6); importantly, biochar affected in different ways PTEs uptake and distribution in hemp. The concentration of Sb (the most abundant PTE in soil) decreased significantly in the roots of plants grown in C + B soil (approx. by 35% compared to those grown on C soil), while Sb concentration in shoots and seeds increased by 24 and 27%, compared to control plants, respectively (Fig. 6A).

The concentration of cationic PTEs increased in roots of cannabis grown in C + B soil (compared to C), i.e. by approx. 14, 32 and 77% for Cd, Pb and Zn respectively (Fig. 6B, C and D). On the contrary, Cd and Zn concentration in shoots decreased for plants grown in C + B soil (i.e., by 24 and 8% respectively) *vs* control plants (Fig. 6B–and D), while Pb concentration substantially increased (~87%). Also, PTEs concentration in seeds was significantly affected by biochar, i.e. Cd and Pb concentrations in seeds of plants grown in C + B were under the detection limit (<0.2 μg kg^{-1}), while those of control plants were 0.12 and 1.09 mg kg^{-1} for Cd and Pb respectively (Fig. 6B and C). On the other hand, biochar addition did not affect Zn concentration in seeds (Fig. 6D).

Overall, these results show for the first time that biochar can significantly increase hemp phytostabilisation potentials with respect to Cd, Pb and Zn. At the same time, biochar revealed very active at increasing hemp phytoextracting capacity with respect to Sb. This could be explained by a biochar-mediated improvement of the soil physico-chemical environment which eventually led to a better plant growth (Fig. S2) and a possible metabolic adaptation of hemp (to the harsh environment) which favoured PTEs uptake and/or their translocation [62].

3.8. Influence of biochar on PTE mineralomasses (MM) of hemp

The plant removal efficiency of the different PTEs present in soil can be estimated by mineralomasses (MM_R, MM_A and MM_S), which quantify the total PTEs amounts actually bioaccumulated in the different plant tissues [40]. The highest mineralomasses were recorded for shoots, the only exception was Pb, where MM_R values were higher than MM_A and MM_S (Table S5). Although PTEs were preferentially stored at root level (except Sb; Fig. 6), the higher shoot biomass resulted in higher MM_A values.

Biochar addition significantly increased PTEs-MM_R (except Sb which was unaffected) by a minimum of ~1.6-fold for Cd up to a maximum of ~2.5-fold for Zn (Table S5). The same was observed for PTEs-MM_A (with no exception) which increased by a minimum of ~1.3-fold for Cd up to a maximum ~3.2-fold for Pb. Regarding Sb, which was the main contaminant in soil, MM_A increased by ~2.1-fold in the biochar-amended soil. Finally, MM_S increased in C + B only for Sb (~2.5-fold) and Zn (~2.0-fold; Table S5). These data clearly highlight that, although biochar decreased the mobility of labile PTEs in soil (mostly Sb), it also resulted in a higher PTEs absorption by hemp. As previously mentioned, this was likely due to better physico-chemical and microbial characteristics in biochar-amended soil which stimulated plant growth and PTEs absorption by the plant [40,63]. Mineralomasses data finally confirmed that biochar can be a suitable amendment for the assisted-phytoremediation of Sb-rich PTEs-contaminated soils by using hemp. In particular, biochar increased the amount of PTEs stabilized in roots as well as that stored in the aerial biomass. Considering that this latter should be harvested to produce bioenergy (or other valuable products, e.g. fibers and oil), an additional relevant amount of PTEs would be removed from soil contributing to its recovery.

4. Conclusions

In this study we showed that softwood biochar can be used in assisted phytoremediation programs of Sb-rich and PTEs-contaminated soils using hemp. Biochar was able to reduce labile Sb and increase residual PTEs in the contaminated soil and improve selected soil chemical attributes. Biochar also increased soil microbial abundance, diversity and functionality (e.g., soil basal respiration), while hemp biomass (i.e. shoots and seeds) increased in the presence of biochar. Such increased hemp growth was accompanied by removal of PTEs, and their higher storage in roots, shoots and seeds. Overall, these results offer a new possibility for the use of PTEs-contaminated soils which foresees a reduction of environmental risks and income generation due to valuable biomass exploitation. For instance, hemp straw can be used for anaerobic digestion and/or incineration to produce electricity and heat, while refined products can be obtained from seeds. Using biochar and hemp for phytoremediation of PTEs-contaminated soils can be therefore an attractive win-win strategy to convert unproductive areas into productive farmland, while reducing at the same time their environmental impact and potential health risks. However, such perspective should be further explored and validated in different environments (especially *in situ* evaluations are needed) and different soil types contaminated by a wider range of PTEs. For instance, the growth of hemp (especially of the root system) is somehow restricted in pots and therefore, the results obtained in this study will need to be supported by future field trials. Other studies should be also addressed to identify hemp varieties that are better adapted to PTEs-pollutes environments.

Funding sources

This research was supported by the Agritech National Research Center and received funding from the European Union Next-GenerationEU (PIANO NAZIONALE DI RIPRESA E RESILIENZA (PNRR) – MISSIONE 4 COMPONENTE 2, INVESTIMENTO 1.4 – D. D. 1032 June 17, 2022, CN00000022). This manuscript reflects only the authors' views and opinions, neither the European Union nor the European Commission can be considered responsible for them.

This research was also supported by the Fondazione di Sardegna (Bando competitivo Fondazione di Sardegna – 2017 per progetti di ricerca con revisione tra pari "Impiego del biochar come ammendante per il recupero fisico, chimico e biologico di suoli contaminati da antimonio").

Data availability

Data are included in the supplementary material.

CRediT authorship contribution statement

Matteo Garau: Writing – original draft, Investigation, Formal analysis. **Mauro Lo Cascio:** Writing – original draft, Investigation, Formal analysis. **Sotirios Vasileiadis:** Formal analysis, Data curation. **Tom Sizmur:** Formal analysis. **Maria Nieddu:** Formal analysis, Data curation. **Maria Vittoria Pinna:** Methodology, Investigation, Data curation. **Costantino Sirca:** Resources, Data curation. **Donatella Spano:** Resources. **Pier Paolo Roggero:** Writing – review & editing, Data curation. **Giovanni Garau:** Writing – review & editing, Resources, Methodology, Conceptualization. **Paola Castaldi:** Writing – review & editing, Supervision, Resources, Methodology, Data curation, Conceptualization.

Declaration of competing interest

The authors declare that they have no known competing financial interests or personal relationships that could have appeared to influence the work reported in this paper.

Appendix A. Supplementary data

Supplementary data to this article can be found online at https://doi.org/10.1016/j.heliyon.2024.e28050.

References

[1] M.A. Destek, A. Aslan, Renewable and non-renewable energy consumption and economic growth in emerging economies: evidence from bootstrap panel causality, Renew. Energy 111 (2017) 757–763, https://doi.org/10.1016/j.renene.2017.05.008.
[2] M. van Dijk, T. Morley, M.L. Rau, Y. Saghai, A meta-analysis of projected global food demand and population at risk of hunger for the period 2010–2050, Nat. Food 2 (2021) 494–501, https://doi.org/10.1038/s43016-021-00322-9.
[3] G. Todde, G. Carboni, S. Marras, M. Caria, C. Sirca, Industrial hemp (*Cannabis sativa* L.) for phytoremediation: energy and environmental life cycle assessment of using contaminated biomass as an energy resource, Sustain. Energy Technol. Assessments 52 (2022) 102081, https://doi.org/10.1016/j.seta.2022.102081.
[4] M.T. Enyigwe, O.S. Onwuka, J.C. Egbueri, Geochemical distribution, statistical and health risk assessment of toxic elements in groundwater from a typical mining district in Nigeria, Environ. Forensics 23 (5–6) (2022) 469–481, https://doi.org/10.1080/15275922.2021.1907822.
[5] H. Tang, G. Meng, J. Xiang, A. Mahmood, G. Xiang, S. Ullah, Y. Liu, G. Huang, Toxic effects of antimony in plants: reasons and remediation possibilities-A review and future prospects, Front. Plant Sci. 13 (2022) 1011945, https://doi.org/10.3389/fpls.2022.1011945.
[6] G. Garau, M. Silvetti, S. Vasileiadis, E. Donner, S. Diquattro, S. Deiana, E. Lombi, P. Castaldi, Use of municipal solid wastes for chemical and microbiological recovery of soils contaminated with metal (loid)s, Soil Biol. Biochem. 111 (2017) 25–35, https://doi.org/10.1016/j.soilbio.2017.03.014.
[7] S.P. Sohi, E. Krull, E. Lopez-Capel, R. Bol, A review of biochar and its use and function in soil, Adv. Agron. 105 (2010) 47–82, https://doi.org/10.1016/S0065-2113(10)05002-9.
[8] M.V. Pinna, G.P. Lauro, S. Diquattro, M. Garau, C. Senette, P. Castaldi, G. Garau, Softwood-derived biochar as a green material for the recovery of environmental media contaminated with potentially toxic elements, Water Air Soil Pollut. 233 (5) (2022) 1–17, https://doi.org/10.1007/s11270-022-05616-7.
[9] Y. Zhu, J. Yang, L. Wang, Z. Lin, J. Dai, R. Wang, Y. Yu, H. Liu, C. Rensing, R. Feng, Factors influencing the uptake and speciation transformation of antimony in the soil-plant system, and the redistribution and toxicity of antimony in plants, Sci. Total Environ. 738 (2020) 140232, https://doi.org/10.1016/j.scitotenv.2020.140232.
[10] X. Jia, J. Zhou, J. Liu, P. Liu, L. Yu, B. Wen, Y. Feng, The antimony sorption and transport mechanisms in removal experiment by Mn-coated biochar, Sci. Total Environ. 724 (2020) 138158, https://doi.org/10.1016/j.scitotenv.2020.138158.
[11] Y.Y. Wang, H.Y. Ji, H.H. Lyu, Y.X. Liu, L.L. He, L.C. You, C.H. Zhou, S.M. Yang, Simultaneous alleviation of Sb and Cd availability in contaminated soil and accumulation in Lolium multiflorum Lam, after amendment with Fe–Mn-Modified biochar, J. Clean. Prod. 231 (2019) 556, https://doi.org/10.1016/j.jclepro.2019.04.407.
[12] J. Gu, J. Yao, G. Jordan, B. Roha, N. Min, H. Li, C. Lu, Arundo donax L. stem-derived biochar increases as and Sb toxicities from nonferrous metal mine tailings, Environ. Sci. Pollut. Res. 27 (3) (2020) 2433–2443, https://doi.org/10.1007/s11356-018-2780-x.
[13] A. El-Naggar, S.X. Chang, Y. Cai, Y.H. Lee, J. Wang, S. Wang, C. Ryu, J. Rinklebe, Y.S. Ok, Mechanistic insights into the (im) mobilization of arsenic, cadmium, lead, and zinc in a multi-contaminated soil treated with different biochars, Environ. Int. 56 (2021) 106638, https://doi.org/10.1016/j.envint.2021.106638.
[14] T. Hussain, S.R. Ahmed, A.H. Lahori, M. Mierzwa-Hersztek, V. Vambol, A.A. Khan, L. Rafique, S. Wasia, M.F. Shahid, Z. Zengqiang, In-situ stabilization of potentially toxic elements in two industrial polluted soils ameliorated with rock phosphate-modified biochars, Environ. Pollut. 309 (2022) 119733, https://doi.org/10.1016/j.envpol.2022.119733.
[15] C.C. Tsai, Y.F. Chang, Poultry litter biochar as a gentle soil amendment in multi-contaminated soil: quality evaluation on nutrient preservation and contaminant immobilization, Agronomy 12 (2022) 405, https://doi.org/10.3390/agronomy12020405.
[16] D.F. Placido, C.C. Lee, Potential of industrial hemp for phytoremediation of heavy metals, Plants 11 (2022) 595, https://doi.org/10.3390/plants11050595.
[17] S. Citterio, A. Santagostino, P. Fumagalli, N. Prato, P. Ranalli, S. Sgorbati, Heavy metal tolerance and accumulation of Cd, Cr and Ni by *Cannabis sativa* L, Plant Soil 256 (2) (2003) 243–252, https://doi.org/10.1023/A:1026113905129.
[18] P. Linger, J. Müssig, H. Fischer, J. Kobert, Industrial hemp (*Cannabis sativa* L.) growing on heavy metal contaminated soil: fibre quality and phytoremediation potential, Ind. Crops Prod. 6 (1) (2002) 33–42, https://doi.org/10.1016/S0926-6690(02)00005-5.

[19] G. Deng, M. Yang, M.H. Saleem, M. Rehman, S. Fahad, Y. Yang, M.S. Elshikhd, J. Alkahtani, S. Ali, S.M. Khan, Nitrogen fertilizer ameliorate the remedial capacity of industrial hemp (*Cannabis sativa* L.) grown in lead contaminated soil, J. Plant Nutr. 44 (12) (2021) 1770–1778, https://doi.org/10.1080/01904167.2021.1881553.

[20] E. Meers, A. Ruttens, M. Hopgood, E. Lesage, F.M.G. Tack, Potential of Brassic rapa, Cannabis sativa, Helianthus annuus and Zea mays for phytoextraction of heavy metals from calcareous dredged sediment derived soils, Chemosphere 61 (4) (2005) 561–572, https://doi.org/10.1016/j.chemosphere.2005.02.026.

[21] M. Ćaćić, A. Perčin, Ž. Zgorelec, I. Kisić, Evaluation of heavy metals accumulation potential of hemp (*Cannabis sativa* L.), J. Cent. Eur. Agric. 20 (2) (2019) 700–711, https://doi.org/10.5513/JCEA01/20.2.2201.

[22] R. Cidu, R. Biddau, E. Dore, A. Vacca, L. Marini, Antimony in the soil–water–plant system at the Su Suergiu abandoned mine (Sardinia, Italy): strategies to mitigate contamination, Sci. Total Environ. 497 (2014) 319–331, https://doi.org/10.1016/j.scitotenv.2014.07.117.

[23] IUSS Working Group WRB, World Reference Base for Soil Resources. International Soil Classification System for Naming Soils and Creating Legends for Soil Maps, fourth ed., International Union of Soil Sciences (IUSS), Vienna, Austria, 2022, p. 234.

[24] R. Manzano, S. Diquattro, P.P. Roggero, M.V. Pinna, G. Garau, P. Castaldi, Addition of softwood biochar to contaminated soils decreases the mobility, leachability and bioaccesibility of potentially toxic elements, Sci. Total Environ. 739 (2020) 139946, https://doi.org/10.1016/j.scitotenv.2020.139946.

[25] Gazzetta Ufficiale, Metodi ufficiali di analisi chimica dei suoli. DM 13 settembre 1999, suppl. G.U. 248, 21 ottobre 1999 (1999) [Official Journal, Official methods of chemical analysis of soils. Ministerial Decree 13 September 1999, suppl, Official Gazette 248 (21 October 1999 (1999).

[26] D.M. Decreto Ministeriale, 1 marzo 2019 n. 46 - Regolamento relativo agli interventi di bonifica, di ripristino ambientale e di messa in sicurezza, d'emergenza, operativa e permanente, delle aree destinate alla produzione agricola e all'allevamento, ai sensi dell'articolo 241 del decreto legislativo 3 aprile 2006, n. 152 [D. M. Ministerial Decree, 1 March 2019 n.46 - Regulation on the remediation, environmental restoration and safety interventions, emergency, operational and permanent, of areas intended for agricultural production and livestock farming, 3 April 2006 pursuant to Article 241 of Legislative Decree No. 152 of.

[27] W.W. Wenzel, N. Kirchbaumer, T. Prohaska, G. Stingeder, E. Lombi, D.C. Adriano, Arsenic fractionation in soils using an improved sequential extraction procedure, Anal. Chim. Acta 436 (2) (2001) 309–323, https://doi.org/10.1016/S0003-2670(01)00924-2.

[28] S. Diquattro, P. Castaldi, S. Ritch, L. Juhasz, G. Brunetti, K.G. Scheckel, G. Garau, E. Lombi, Insights into the fate of antimony (Sb) in contaminated soils: ageing influence on Sb mobility, bioavailability, bioaccessibility and speciation, Sci. Total Environ. 770 (2021) 145354, https://doi.org/10.1016/j.scitotenv.2021.145354.

[29] N. Basta, R. Gradwohl, Estimation of Cd, Pb, and Zn bioavailability in smelter-contaminated soils by a sequential extraction procedure, J. Soil Contam. 9 (2) (2000) 149–164, https://doi.org/10.1080/10588330008984181.

[30] M. Garau, G. Garau, S. Diquattro, P.P. Roggero, P. Castaldi, Mobility, bioaccessibility and toxicity of potentially toxic elements in a contaminated soil treated with municipal solid waste compost, Ecotoxicol. Environ. Saf. 186 (2019) 109766, https://doi.org/10.1016/j.ecoenv.2019.109766.

[31] K. Alef, P. Nannipieri, Enzyme activities, in: K. Alef, P. Nannipieri (Eds.), Methods in Applied Soil Microbiology and Biochemistry, first ed., 1995, pp. 311–373, https://doi.org/10.4236/wjet.2017.53B011.

[32] S. Chahine, G. Garau, P. Castaldi, M.V. Pinna, S. Melito, G. Seddaiu, P.P. Roggero, Stabilising fuoride in contaminated soils with monocalcium phosphate and municipal solid waste compost: microbial, biochemical and. plant growth impact, Environ. Sci. Pollut. Res. 29 (27) (2022) 41820–41833, https://doi.org/10.1007/s11356-021-17835-2.

[33] L. Chessa, A. Pusino, G. Garau, N.P. Mangia, M.V. Pinna, Soil microbial response to tetracycline in two different soils amended with cow manure, Environ. Sci. Pollut. Res. 23 (6) (2016) 5807–5817, https://doi.org/10.1007/s11356-015-5789-4.

[34] J.A. Gilbert, J.K. Jansson, R. Knight, Earth microbiome project and global systems biology, mSystems 3 (3) (2018) e00217-17, https://doi.org/10.1128/msystems.00217-17.

[35] W. Walters, E.R. Hyde, D. Berg-Lyons, G. Ackermann, G. Humphrey, A. Parada, J.A. Gilbert, J.K. Jansson, J.G. Caporaso, J.A. Fuhrman, A. Apprill, R. Knight, Improved bacterial 16S rRNA gene (V4 and V4-5) and fungal internal transcribed spacer marker gene primers for microbial community surveys, mSystems 1 (1) (2016) e00009-15, https://doi.org/10.1128/msystems.00009-15.

[36] A.M. Comeau, G.M. Douglas, M.G.I. Langille, Microbiome helper: a custom and streamlined workflow for microbiome research, mSystems 2 (2017) e00127-00116, https://doi.org/10.1128/msystems.00127-16.

[37] B.J. Callahan, P.J. McMurdie, M.J. Rosen, A.W. Han, A.J.A. Johnson, S.P. Holmes, DADA2: high-resolution sample inference from Illumina amplicon data, Nat. Methods 13 (2016) 581–583, https://doi.org/10.1038/nmeth.3869, 10.1038/nmeth.3869.

[38] B. Callahan, K. Sankaran, J. Fukuyama, P. McMurdie, S. Holmes, Bioconductor workflow for microbiome data analysis: from raw reads to community analyses, F1000Research (2016), https://doi.org/10.12688/f1000research.8986.2, 510.12688/f1000research.8986.2.

[39] P. Yilmaz, L.W. Parfrey, P. Yarza, J. Gerken, E. Pruesse, C. Quast, T. Schweer, J. Peplies, W. Ludwig, F.O. Glöckner, The SILVA and "all-species living tree project (LTP)" taxonomic frameworks, Nucleic Acids Res. 42 (2014) D643–D648, https://doi.org/10.1093/nar/gkt1209, 10.1093/nar/gkt1209.

[40] M. Lebrun, F. Miard, R. Nandillon, N. Hattab-Hambli, G.S. Scippa, S. Bourgerie, D. Morabito, Eco-restoration of a mine technosol according to biochar particle size and dose application: study of soil physico-chemical properties and phytostabilization capacities of *Salix viminalis*, J. Soils Sediments 18 (6) (2018) 2188–2202, https://doi.org/10.1007/s11368-017-1763-8.

[41] J. Oksanen, G.F. Blanchet, M. Friendly, R. Kindt, P. Legendre, D. McGilinn, P.R. Minchin, R.B. O'Hara, G.L. Simpson, P. Solymos, M. Henry, R. Stevens, E. Szoecs, H. Wagner, Vegan: Community Ecology Package, R Package Version 2.5-7, 2020. https://CRAN.R-project.org/package=vegan(2020.

[42] A. Chao, Estimating the population size for capture-recapture data with unequal catchability, Biometrics 43 (1987) 783–791, https://doi.org/10.2307/2531532.

[43] L. Jost, Entropy and diversity, Oikos 113 (2006) 363–375, https://doi.org/10.1111/j.2006.0030-1299.14714.x.

[44] R.A. Fisher, A.S. Corbet, C.B. Williams, The relation between the number of species and the number of individuals in a random sample of an animal population, J. Anim. Ecol. 12 (1943) 42–58, https://doi.org/10.2307/1411.

[45] A. Rahman, M.M. Rahman, M. Bahar, P. Sanderson, D. Lamb, Transformation of antimonate at the biochar−solution interface, ACS EST Water 9 (2021) 2029–2036, https://doi.org/10.1021/acsestwater.1c00115.

[46] L. Hua, H. Zhang, T. Wei, C. Yang, J. Guo, Effect of biochar on fraction and species of antimony in contaminated soil, J. Soils Sediments 19 (6) (2019) 2836–2849, https://doi.org/10.1007/s11368-019-02251-4.

[47] G. Garau, A. Porceddu, M. Sanna, M. Silvetti, P. Castaldi, Municipal solid wastes as a resource for environmental recovery: impact of water treatment residuals and compost on the microbial and biochemical features of as and trace metal-polluted soils, Ecotoxicol. Environ. Saf. 174 (2019) 445–454, https://doi.org/10.1016/j.ecoenv.2019.03.007.

[48] M. Lo Cascio, L. Morillas, R. Ochoa-Hueso, M. Delgado-Baquerizo, S. Munzi, J. Roales, D. Spano, C. Cruz, A. Gallardo, E. Marnique, M.E. Pérez-Corona, I. Dias, C. Sirca, S. Mereu, Nitrogen deposition effects on soil properties, microbial abundance, and litter decomposition across three shrublands ecosystems from the Mediterranean basin, Front. Environ. Sci. 9 (2021), https://doi.org/10.3389/fenvs.2021.709391.

[49] P. Nannipieri, C. Trasar-Cepeda, R.P. Dick, Soil enzyme activity: a brief history and biochemistry as a basis for appropriate interpretations and meta-analysis, Biol. Fertil. Soils 54 (1) (2018) 11–19, https://doi.org/10.1007/s00374-017-1245-6.

[50] W. Demisie, Z. Liu, M. Zhang, Effect of biochar on carbon fractions and enzyme activity of red soil, Catena 121 (2014) 214–221, https://doi.org/10.1016/j.catena.2014.05.020.

[51] M.N. Khan, J. Huang, D. Li, N.A. Daba, T. Han, J. Du, M. Qaswar, C.K. Antonio, T.A. Sial, L. Zhang, Y. Xu, Z. He, H. Zhang, A. Núñez-Delgado, Mitigation of greenhouse gas emissions from a red acidic soil by using magnesium-modified wheat straw biochar, Environ. Res. 203 (2022) 111879, https://doi.org/10.1186/s12284-023-00638-z.

[52] A. Ali, S.M. Shaheen, D. Guo, Y. Li, R. Xiao, F. Wahid, M. Azeem, K. Sohail, T. Zhang, J. Rinklebe, R. Li, Z. Zhang, Apricot shell-and apple tree-derived biochar affect the fractionation and bioavailability of Zn and Cd as well as the microbial activity in smelter contaminated soil, Environ. Pollut. 264 (2020) 114773, https://doi.org/10.1016/j.envpol.2020.114773.

[53] A. Kaurin, Z. Cernilogar, D. Lestan, Revitalisation of metal-contaminated, EDTA-washed soil by addition of unpolluted soil, compost and biochar: effects on soil enzyme activity, microbial community composition and abundance, Chemosphere 193 (2018) 726–736, https://doi.org/10.1016/j.chemosphere.2017.11.082.
[54] R. Cardelli, M. Becagli, F. Marchini, A. Saviozzi, Biochar impact on the estimation of the colorimetric-based enzymatic assays of soil, Soil Use Manag. 35 (3) (2019) 478–481, https://doi.org/10.1111/sum.12533.
[55] B. Tang, H. Xu, F. Song, H. Ge, L. Chen, S. Yue, W. Yang, Effect of biochar on immobilization remediation of Cd- contaminated soil and environmental quality, Environ. Res. 204 (2022) 111840, https://doi.org/10.1016/j.envres.2021.111840.
[56] B. Maestrini, P. Nannipieri, S. Abiven, A meta-analysis on pyrogenic organic matter induced priming effect, GCB Bioenergy 7 (4) (2015) 577–590, https://doi.org/10.1111/gcbb.12194.
[57] M.J, R.N. Anderson, K.R. Gorley, Clarke, PERMANOVA+ for PRIMER: Guide to Software and Statistical Methods, PRIMER-E, Plymouth, UK, 2008.
[58] S.D. Siciliano, A.S. Palmer, T. Winsley, E. Lamb, A. Bissett, M.V. Brown, J. van Dorst, M. Ji, B.C. Ferrari, P. Grogan, H. Chu, I. Snape, Soil fertility is associated with fungal and bacterial richness, whereas pH is associated with community composition in polar soil microbial communities, Soil Biol. Biochem. 78 (2014) 10–20, https://doi.org/10.1016/j.soilbio.2014.07.005.
[59] K. Choi, R. Khan, S. Lee, Dissection of plant microbiota and plant-microbiome interactions, J. Microbiol. 59 (2021) 281–291, https://doi.org/10.1007/s12275-021-0619-5.
[60] S.L. Cosentino, E. Riggi, G. Testa, D. Scordia, V. Copani, Evaluation of European developed fibre hemp genotypes (*Cannabis sativa* L.) in semi-arid Mediterranean environment, Ind. Crops Prod. 50 (2013) 312–324, https://doi.org/10.1016/j.indcrop.2013.07.059.
[61] M. Flajšman, D.K. Ačko, Influence of edaphoclimatic conditions on stem production and stem morphological characteristics of 10 European hemp (*Cannabis sativa* L.) varieties, Acta Agric. Slov. 115 (2) (2020) 399–407, https://doi.org/10.14720/aas.2020.115.2.1528.
[62] E. Loffredo, G. Picca, M. Parlavecchia, Single and combined use of *Cannabis sativa* L. and carbon-rich materials for the removal of pesticides and endocrine-disrupting chemicals from water and soil, Environ. Sci. Pollut. Res. 28 (3) (2021) 3601–3616, https://doi.org/10.1007/s11356-020-10690-7.
[63] M. Garau, G. Garau, T. Sizmur, S. Coole, P. Castaldi, M.V. Pinna, Biochar and Eisenia fetida (Savigny) promote sorghum growth and the immobilization of potentially toxic elements in contaminated soils, Appl. Soil Ecol. 182 (2023) 104697, https://doi.org/10.1016/j.apsoil.2022.104697.